8444 J. Agric. Food Chem. 2010, 58, 8444–8452
DOI:10.1021/jf101063m

JOURNAL OF AGRICULTURAL AND FOOD CHEMISTRY
ARTICLE

Starch Digestion Mechanistic Information from the Time Evolution of Molecular Size Distributions

Torsten Witt, Michael J. Gidley, and Robert G. Gilbert*

School of Land Crop & Food Sciences, Centre for Nutrition & Food Sciences, The University of Queensland, Brisbane, Qld 4072, Australia

Size-exclusion chromatography [SEC, also termed gel permeation chromatography (GPC)] is used to measure the time evolution of the distributions of molecular size and of branch length as starch is subjected to in vitro digestion, including studying the development of enzyme-resistant starch. The method is applied to maize starches with varying amylose contents; the starches were extruded so as to provide an analogue for processed food. The initial rates of digestion of amylose and amylopectin components were found to be the same for high-amylose starches. A small starch species, not present in the original starting material, was formed during the digestion process; this new species has a slower digestion rate and is probably formed by retrogradation of longer branches of amylose and amylopectin as they are partially or wholly liberated from their parent starch molecule during the digestion process. The data suggest that the well-known connection between high amylose content and resistant starch arises from the greater number of longer branches, which can form the small retrograded species. The method is useful for the purpose of comparisons between different starches undergoing the process of digestion, by observing the changes in their molecular structures, as an adjunct to detailed studies of the enzyme-resistant fraction.

KEYWORDS: Resistant starch; size exclusion chromatography; digestibility; molecular weight distribution; gel permeation chromatography; maize; amylose

INTRODUCTION

Starch is a composite of two glucose homopolymers, amylose and amylopectin (*1*). Amylose is of moderate molecular weight ($\sim 10^6$) with a few long-chain branches, and amylopectin is a hyperbranched polymer with extremely high molecular weights. Approximately 20−50% of human food energy comes directly from the consumption of starch (*2*). The risk factors for nutrition-related diseases such as obesity, diabetes, and colorectal cancers probably contain aspects of starch structure, and thus, improved understanding of the process of starch digestion is of considerable importance (*3*).

The rate of digestion of starch by amylases in the digestive tract depends on the physical form and chemical structure of the starches as eaten. Following initial hydrolysis by α-amylase (initially in saliva and more extensively in the small intestine), oligomeric fragments are rapidly converted to glucose by enzymes such as maltase-glucoamylase and sucrase-isomaltase (for which the fungal enzyme amyloglucosidase is an easily available analogue) and taken up into circulation (*4*). A high digestion rate leads to a rapid rise in plasma glucose, which the body attempts to control with an insulin "spike"; repetition of this process is thought to be a major risk factor for maturity-onset diabetes and other manifestations of metabolic syndrome. Resistant starch is a species of particular interest due to its link to the prevention of colorectal cancer (*3*), causing decreases in peak glucose and insulin responses of importance for diabetes (*5*−*7*), as well as potentially increasing levels of satiety (*8*).

The rate of starch digestion in vitro has been separated into three arbitrary categories (*9*): rapidly digested starch (RDS, digested in under 20 min), slowly digested starch (SDS, digested between 20 min and 2 h), and resistant starch (RS, any starch still being digested after 2 h). These categories have been adopted for ease of comparison, although the physiological digestion of starch is significantly more complex. Resistant starch itself can be subdivided into several categories, RS1−4 (*10*). RS3 is starch that has had its granular structure completely disrupted, typically via gelatinization, but is resistant due to retrogradation effects and is the most relevant type of resistant starch in human consumption of cooked/processed foods. The digestion times assigned to RDS, SDS, and RS should not be interpreted as having direct physiological relevance, but this categorization is a convenient laboratory approach for comparing different starches (*11*).

There is a well-known correlation between an increase in amylose content and an increase in RS3 resistant starch (*12*, *13*). RS3 is considered to include starch helices that are inaccessible to digestive enzymes (*14*). The average length of chains (branches) in the helices ranges from a degree of polymerization (DP) of 20 to 40 glucose monomers (*14*−*16*). The analyses used for these inferences have, however, all been performed at the end point of the digestion, when there is only the resistant starch residue species; there is, as yet, no clear view of the progression of starch digestion and the formation of resistant starch (*17*). Indeed, "resistant starch" is further hydrolyzed with continued digestion (*18*).

*To whom correspondence should be addressed. Tel: +61 7 3365 409. Fax: +61 7 3365 1188. E-mail: b.gilbert@uq.edu.au.

 Published on Web 06/24/2010

Bertoft et al. observed the effect of α-amylase on a variety of granular starches such as potato (*19*), waxy maize (*20*), barley (*21*), and waxy rice (*22*). The Englyst method (*9*), or variations on it, is a common in vitro method to simulate mammalian digestion; Hernandez et al. used it to observe the digestion of starch films (*23*); Kumari et al. used it to observe resistant starch formation with lengthy storage times (*24*); Osorio-Diaz et al. observed the differences in digestibility between canned and dried beans (*25*); and Lopez-Rubio et al. observed the changes caused to starch nanostructure by digestion and extrusion (*26*). Zhang et al. showed that the slowly digestible properties are due to amylopectin structure containing either high proportions of short or long branching chains (*27*); more specifically, the short chain branches, and therefore a larger number of branches, are unfavorable for α-amylolysis. In the case of a higher proportion of long chains (particularly longer amylopectin chains), the starch is more likely to undergo significant retrogradation, including the production of starch helices, which cause slower digestion (*28*). Jiang et al. observed the production of RS, including the production of a small, 59−74 DP, linear resistant starch species and a larger, 840−951 DP, branched structure (*29*). The species that remains after starch digestion in vitro, enzyme-resistant starch (*11*), has been studied by Eerlingen et al., who found that regardless of amylose source a similar end product, a linear starch chain of 19−26 DP, was formed (*16*). Evans et al. (*30*) examined the digestion of high amylose maize starch and found that the kinetic process of enzyme-resistant starch production could be divided into two different rates, which they hypothesized was due to different species being present at different times of the digestion. There are extensive data in the literature on α-limit (*19*) dextrins, which are formed by the action of α-amylase on starch over an extended time period. Zhu et al. (*19*) reported DPs for dextrins produced from potato after 5 h of α-amylase digestion ranging from 1 to 1000; further α-amylolysis reduced the α-limit dextrins to branched DP 30−70 clusters. Poutannen et al. (*31*) found that α-amylolysis produced predominately branched molecules that reduce in size with time. Bertoft et al. (*32*) found α-amylolysis produced maltohexaose and branched α-dextrins, which also decreased in size with time. The product from initial α-amylase attack was found to have a broad distribution of DP from 2 to 500 and produced both linear and branched products from both amylose and amylopectin (*33*).

These studies are complementary to the present one, which examines the in vitro digestion of four maize starches of varying amylose contents, to see what mechanistic information on the digestive process can be gleaned from changes in the size distributions of whole and debranched starches. The starches are extruded, to mimic food processing, which includes gelatinization. The size distributions of the starch digests at different times are obtained using size exclusion chromatography [SEC, also known as gel permeation chromatography (GPC)].

MATERIALS AND METHODS

Starches were provided by Penford Food Ingredients Co.: Gelose 80, Gelose 50, regular maize starch (rms), and a waxy maize starch; Gelose 50 and Gelose 80 were convenient commercial sources of starch with greatly elevated amylose content and thus suitable for examining effects resulting from longer branches. The amylose contents were determined by Tan et al. using the iodine binding method (*34*); Gelose 80 and Gelose 50 were high-amylose starches with 82.9 and 56.3% apparent amylose contents, respectively; the rms used here had an apparent amylose content of 24.4%, while the waxy maize had 3.4% apparent amylose content.

Extrusion Process. The water content in each starch was measured using AOAC method 925.09 six times for each starch variety, and the results were averaged. Extrusion was performed on a Prism Eurolab Digital from Thermo Scientific (Waltham, United States) twin-screw extruder using a 3 mm circular die. All four starches were run at constant moisture content, temperature profile, total flow rate, and screw speed. The moisture content of the extrudate varied from 27.5 to 28% and had a total flow rate of 1.526 kg h^{-1}; the screw speed was set at 180 rpm, and values for barrel temperature are given in **Table 1**. After the temperature stabilized and a consistent product was observed, extrusion was continued for a further 15−20 min to ensure that a steady state had been reached before approximately 50 g of extrudate was collected. After extrusion, all samples were left at room temperature for more than a week.

Table 1. Extruder Barrel Temperatures

barrel chamber	1	2	3	4	5	6	7	8	9	10
temperature (°C)	50	75	100	120	120	110	105	100	95	−

After extrusion and storage at room temperature, the starches were freeze-dried using a Christ Alpha 1−4 LSC freeze dryer (Osterhode am Harz, Germany) overnight in preparation for cryogrinding. Extruded samples were then ground using a Spex Sampleprep 6850 Freezer/Mill (Metuchen, United States). Cryogrinding consisted of a 10 min precooling period followed by two 5 min grinding periods separated by a 2 min intercooling period. The grinding intensity was set to 10 Hz. The resulting powder was passed through a Labtechnics (Kilkenny, Australia) 250 μm sieve and then stored in a desiccator until it was used for digestion experiments.

Digestion. The method of digestion was a variation on the procedure described by Htoon et al. (*18*), which simulates digestion in three steps: salival digestion, stomach digestion, and intestinal digestion. While this procedure is by no means a precise mimic of the complex (and heterogeneous) processes involved in human digestion, there is acceptable evidence (*35*,*36*) that it does mimic the ranking of the digestion rates of different starches, even though the actual rates may be different from those in humans. The following solutions were prepared prior to the digestion: carbonate buffer at pH 7; sodium acetate buffer, pH 6.0; artificial saliva solution using porcine pancreas α-amylase (Sigma Aldrich); artificial stomach solution, pH 2.0, including gastric porcine mucosa pepsin (Sigma Aldrich); small intestinal solution including porcine pancreas pancreatin (Sigma Aldrich); and *Aspergillus niger* amyloglucosidase (Megazyme, Bray, Ireland).

The samples comprised 500 mg of extruded starch. The salival solution was added to the starch for 30 s, followed by the stomach solution, which was then incubated for 30 min in an oscillating water bath at 37 °C at 85 rpm. After this, the solution was neutralized, and the intestinal solution was added; at this point, the "0 h" samples were removed, and all other solutions were incubated again for varying lengths of time: 0.5, 1, 2, 4, 8, and 24 h. The differences between digestions can be seen in terms of RDS, SDS, and RS as defined in the introduction: The undigested extruded sample is the baseline, 0−0.5 h can be considered as RDS; 0.5−2 h as SDS; and 2−24 h as RS. After samples were removed, they were rapidly frozen using a dry ice/acetone mixture and stored; at a later time, samples were thawed, and the starch solution was washed several times with ethanol to remove protein and glucose. Samples were refrozen, freeze-dried, weighed for yield, and stored in a desiccator.

Debranching of Starch. Debranching was done using a variation of the technique described by O'Shea et al. (*37*); the fluorophore attachment step of O'Shea et al. was not required because fluorescence detection was not used. A 20 mg sample of each sample was used for debranching; this included the seven sampling times plus the extrudate of each of the four maize starches. The debranching was performed using iso-amylase from Megazyme (Wicklow, Ireland). After they were debranched, the samples were frozen, freeze-dried, and stored in a desiccator until ready for use.

SEC. SEC was performed on a PSS (Mainz, Germany) Agilent 1100 series using a Shimadzu RID-10A refractive index detector. For whole-molecule distributions, samples were prepared using 2 mg mL^{-1} starch in dimethylsulfoxide (DMSO) with 0.5% LiBr, a solvent combination that completely dissolves even high-amylose starches with minimal degradation (*38*). Samples were injected into the following series of PSS columns: precolumn, Gram10000, and Gram1000. The injection volume was 100 μL, the flow rate was 0.3 mL min^{-1}, and the temperature was 80 °C.

While fluorophore-assisted capillary electrophoresis (FACE) (*37*,*39*) is ideally suited to accurately analyze debranched amylopectin, it has an insufficient size range to analyze the longer chains of debranched amylose;

thus, SEC is used here for the debranched-molecule distributions. Although amylopectin suffers shear degradation in SEC (*40*), the goals of the present work are such that this does not pose a problem, due to the comparative and semiquantitative nature of the study.

Debranched samples comprised 2 mg mL^{-1} starch in DMSO with 0.5% LiBr and were injected into two PSS Gram100 columns following a precolumn. The injection volume was 100 μL, the flow rate was 0.9 mL s^{-1}, and the temperature was 80 °C. All data were collected using WinGPC software.

SEC separates by hydrodynamic volume, V_h, not by molecular weight. For linear polymers (including debranched starch), there is a unqiue relation between molecular weight M (or DP, X) and V_h. This is not the case for a branched polymer such as starch, because two starch molecules with the same size can have different branching structures and thus different molecular weights. SEC data for whole (undebranched) starches are presented here in terms of hydrodynamic radius R_h, related to V_h by $V_h = 4/3\ \pi\ R_h^3$. To implement this, the relation between the molecular weights of the (linear) pullulan standards and V_h was obtained using the assumption of universal calibration and pullulan standards, as described elsewhere (*40*). The Mark−Houwink parameters for pullulan were those quoted by Cave et al. (*40*). Because of shear scission in SEC and the limitations of the available size of the pullulan standards, the size axis for the amylopectin region, corresponding to $R_h \gtrsim 50$ nm for the present conditions, is only semiquantitative. These limitations do not present any difficulties for the purposes of this paper, whose goal is mechanistic interpretation, for which purpose a semiquantitative examination of trends is sufficient. For branched polymers, the size distribution is presented as the weight SEC distribution, $w(\log R_h)$, which is the weight of chains in the volume increment between $\log R_h$ and $\log R_h + d(\log R_h)$. The $w(\log R_h)$ has been normalized to the percentage of yield remaining for each sample. The weight distribution in terms of hydrodynamic volume, $w(\log V_h)$, is proportional to $w(\log R_h)$.

For linear (e.g., debranched) polymers, there is a unique relation between molecular weight M and V_h. Data for these samples are thus presented in terms of both R_h and M. However, for the very smallest molecular weights of the debranched chains, the Mark−Houwink relation, and hence the lower range of M, may not be quantitatively accurate (e.g., see ref *41*).

RESULTS AND DISCUSSION

The yields produced during digestion are presented in **Figure 1**. These data show the process of digestion occurring rapidly in the first 4 h, after which the rate of digestion decreases and tends toward complete digestion. A 10 mg portion of the Gelose 80 and Gelose 50 24 h samples was subjected to a week of digestion using digestion enzymes from the intestinal digestion stage, at the end of which there was no longer any visible starch residue. This was used as a rough indicator that the starch had not become completely enzyme-resistant and still underwent digestion. The amount of starch digested correlates with the amount of amylose: that is, starches with higher amounts of amylose were less digested at a particular time than starches with higher amounts of amylopectin. Specifically, Gelose 80, with the highest apparent amylose content, underwent the least digestion, while the waxy starch, with minimal amylose content, was almost completely digested after 3 h, resulting in less than 1% of the starch remaining. Evans et al. (*30*) conducted a similar experiment and obtained kinetic information from the system; we use a similar method of plotting $\log_{10}$(% starch remaining) vs time, as shown in **Figure 1**. While the kinetics do not follow a simple first-order behavior [linear log(concentration) vs time], there is a trend of reaction rates decreasing with an increase in amylose content, which is present in both the initial rapid digestion and the later digestion rate; on the other hand, the waxy maize shows a constant rate [linear log(concentration) vs time] for the duration of its digestion.

The size distributions for all of the starches are presented as both three-dimensional plots (**Figure 2** for the whole molecule distribution and **Figure 3** for the debranched distributions) and

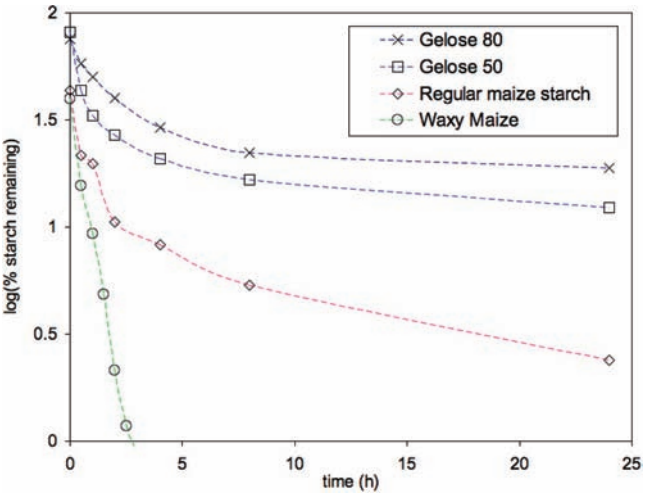

Figure 1. Digestion yields of maize starches as a function of time, as $\log_{10}$(% starch remaining); this would be linear if first-order kinetics were obeyed. Dashed lines joining the points are only for visual guidance.

overlaid two-dimensional plots (**Figures 4**−**7**) for the four types of starches and for successive digestion times. The reason that the same data are presented as both three- and two-dimensional plots is that the former representation is better for perceiving overall trends, while the latter enables semiquantitative features to be distinguished (particularly the appearance of a new size component at small R_h). These figures show $w(\log R_h)$ as a function of both R_h (on a log scale) and digestion time. The two-dimensional plots of the debranched distributions have an additional axis showing the DP (recall that size and DP are uniquely related only for linear polymers such as debranched starch). In these figures, "extrudate" refers to the starch sample after processing but before undergoing any kind of digestion, while the time lengths refer to the time spent in the intestinal digestion step.

Distributions of Extrudate Prior to Digestion. The focus of the present paper is to see what can be learned from the change in size distributions during digestion. The different starches have rather different distributions prior to digestion, being from a range of native sources. Extrusion has significant effects on the original whole and debranched distributions, for example, see ref (*42*); while the distributions of the extrudate (undigested) starch are not the subject of the present paper, they need some discussion prior to considering their changes with digestion.

All whole-molecule distributions (**Figure 2**) of the extrudates display an amylopectin peak with a hydrodynamic radius of ~75 nm with amylose and any intermediate or extrusion-degraded molecules stretching from 1 to 30 nm; the waxy starch whole-molecule distribution shows only the 75 nm amylopectin peak with no discernible amylose peak. The debranched distributions (**Figure 3**) show the normal qualitative appearance of a bimodal component of small amylopectin branches and a long-chain component corresponding to the branches of amylose. The amylopectin structures of both the regular and the waxy maize starches should be similar, and indeed, they are, as neither is affected by the ae-extender mutation, which affects high-amylose maize starches (*43*). The debranched distribution of the high-amylose, Gelose 80 and Gelose 50, starches shows a much less distinct distribution when compared with rms, as there is significantly more overlap between the amylopectin and the amylose regions of the distribution. This is not because SEC band-broadening (*44*) causes an artifactual merging of peaks: The two components are better separated, showing more distinct regions, for rms. Thus, as has been pointed out before (*45*, *46*), "high-amylose" starches can perhaps be thought of as starches wherein there are a

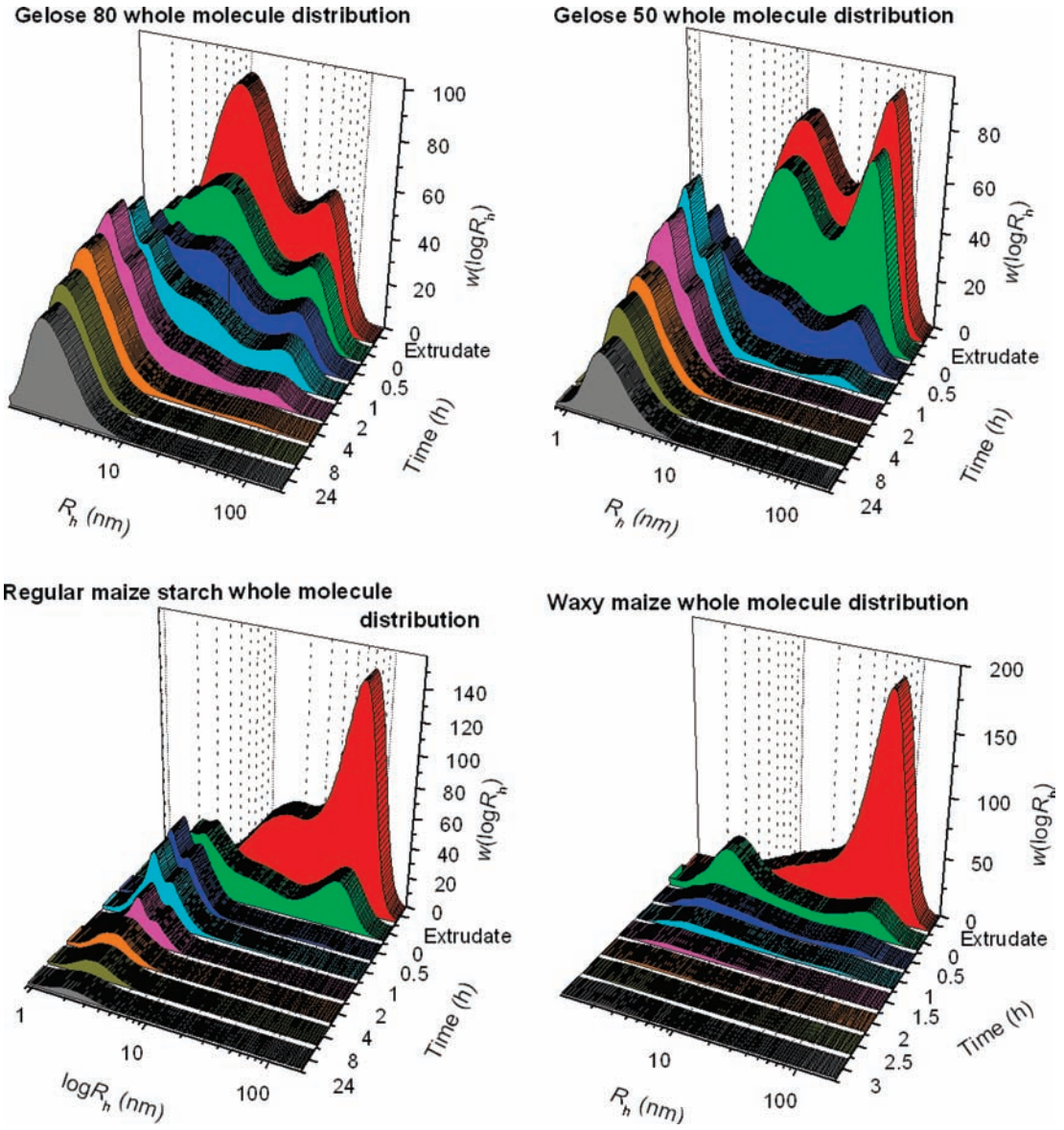

Figure 2. Three-dimensional plots of whole-starch size distributions of four types of starch over successive digestion times.

significant number of longer branches in amylopectin and/or shorter branches in amylose.

Change in Distributions with Digestion. Both amylose and amylopectin components decrease with time, the whole molecule distributions (**Figures 2**) showing a complete loss of both amylopectin and amylose within 2 h, while the debranched distributions (**Figures 3**) show a clear loss only in the longer branches. The detailed whole-starch distributions of **Figures 5**−**7** show an especially interesting feature: the appearance of a separate small-size remnant starch component, whose size, ~ 2 nm, is different from that of both parent amylopectin and parent amylose. Both parent glucans are either rapidly digested to form the new remnant starch species or are digested completely to glucose. The shape of the remnant starch species distribution is relatively symmetric after longer periods of digestion, 4−24 h.

It is seen that the amylopectin component is rapidly digested for regular maize and waxy starches (**Figures 4** and **5**). However, the high-amylose starches, Gelose 50 and Gelose 80 (**Figures 6** and **7**), show slower overall digestion, with the rates of disappearance of amylose and amylopectin being apparently similar. A comparison between the relative rates of disappearance of the whole amylopectin and amylose molecules was made for these high-amylose starches to determine whether there was a preferential digestion of either of the initial molecular species, amylopectin or amylose, by α-amylase or amyloglucosidase, during the early part of the digestion process. The data used for this comprised the Gelose 50 and Gelose 80 whole-molecule distributions (**Figures 6** and **7**), chosen because these show separation between the amylose, the amylopectin, and the remnant starch species peaks over 0−1 h (after which time there is little left of either component for Gelose 50). The relative amounts of amylose and amylopectin were obtained as the ratio of the change in peak heights of each at 0, 0.5, and 1 h to the heights of these in the extrudate, as presented in **Figure 8**. Linear regression (with the line forced to pass through the origin) gives a slope of 0.95 ± 0.01, which is sufficiently close to unity to suggest that the amounts of amylose and amylopectin decrease at the same rate. This suggests that the rate-determining step in the reaction with high-amylose starches is the initial amylolytic attack, after which the products are rapidly digested. There have been a few studies that have shown either a lack of preferential digestion of amylose or amylopectin (*33*, *47*) or a slight preference for amylose digestion (*48*) by bacterial α-amylase in granular starch. It is likely that the increase in digestion rate accompanying decreased amylose content

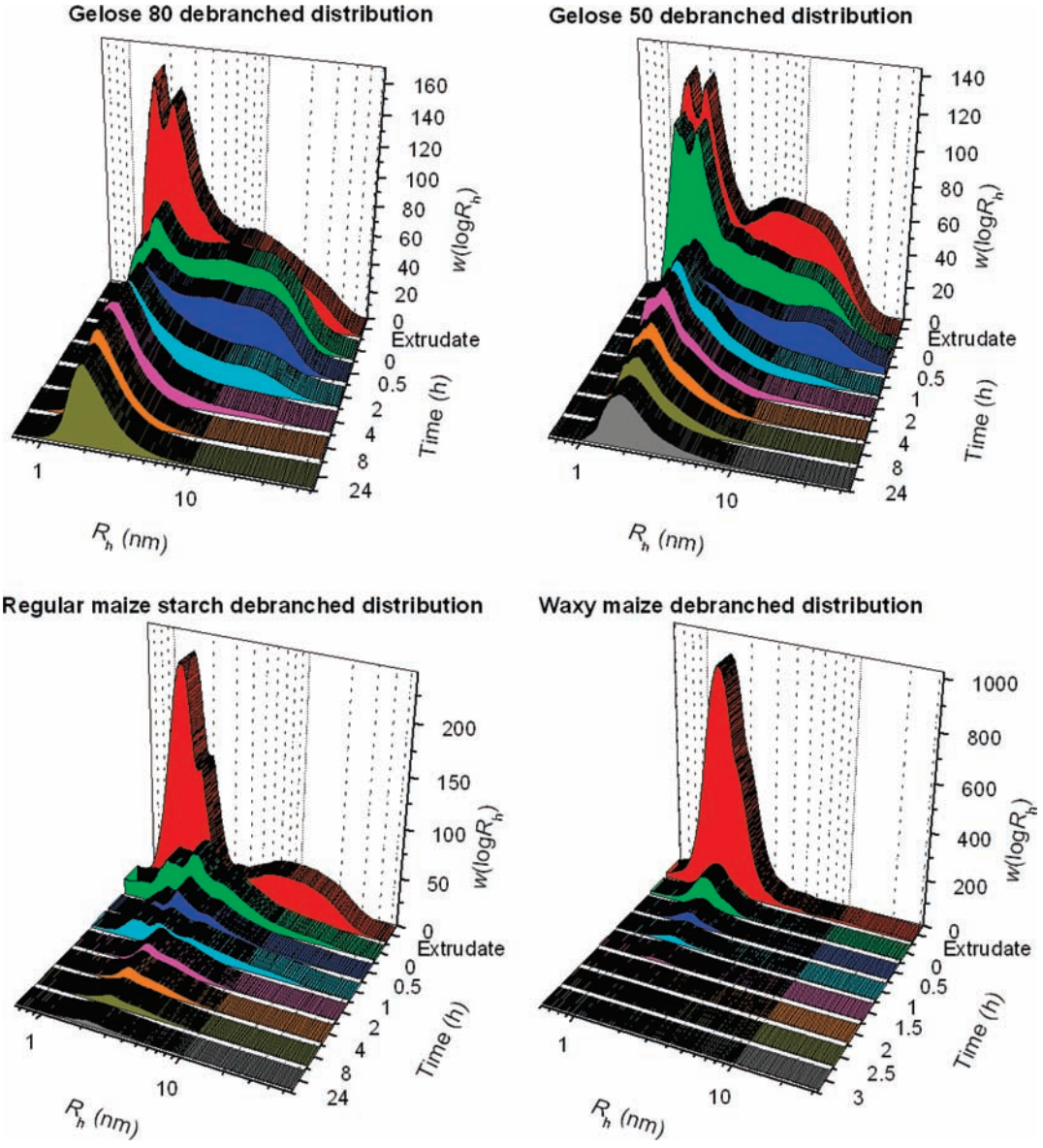

Figure 3. Three-dimensional plots of debranched size distributions of four types of starch over successive digestion times.

in ordinary starches is due, not to a preferential digestion of amylopectin, but to an increase in production of the more slowly digested remnant starch species as seen in this and other studies (*14*−*16*, *30*).

The debranched distributions, **Figures 4**−**7**, show that a gradual loss of structure as the new remnant species is formed. The whole-molecule waxy starch extrudate, **Figure 4**, shows a single large size peak, at ∼75 nm, as expected for a virtually amylopectin-only starch; this is digested over time into a new peak at ∼2−4 nm, whose peak height gradually diminishes in time. The debranched distribution shows a single peak with a shoulder that diminishes in size without changing shape, indicating that the amylopectin present was digested randomly with respect to its branching structure. The debranched peak is at ∼1.5 nm, indicating that the larger structure of the new peak seen in the whole-molecule distribution at 2−4 nm is significantly branched. This indicates that the whole amylopectin molecule is rapidly reduced in size by α-amylase to 2−4 nm fragments and that other fragments are either not produced or that they are rapidly digested via α-amylase and amyloglucosidase in conjunction. The species formed in the waxy maize digestion may be the origin of the slower digestion profile caused by branching as observed by Zhang et al. (*28*).

The whole and debranched distributions of rms are presented in **Figure 5**. At the 0, 0.5, and 1 h time periods, the debranched distributions show a peak at ∼1.5 nm; after this time, they are digested, similar to the behavior of amylopectin shown in the debranched waxy maize distribution, **Figure 4**, which by 1 h has been digested to less than 10% of the original starch present. The remnant species of both the whole and the debranched regular maize distributions are both approximately symmetric with a peak at ∼2 nm, the whole-molecule distribution covering 1−7 nm while the debranched distribution covers from 1 to 8 nm. This similarity of distribution both before and after debranching suggests that, unlike waxy maize, the remnant starch species of rms are predominantly linear.

The whole-molecule distributions of Gelose 80 and Gelose 50 similarly show the production of a remnant starch species at late digestion times, 4−24 h, with a hydrodynamic radius of ∼2 nm, while the debranched distributions produced a similar distribution by 24 h (**Figures 6** and **7**). These 24 h distributions all contain a ∼2 nm peak in both debranched and whole-molecule distributions, which indicates a predominantly linear starch species, while the amylose-free waxy maize has no such distribution. The debranched distribution of Gelose 80 becomes approximately

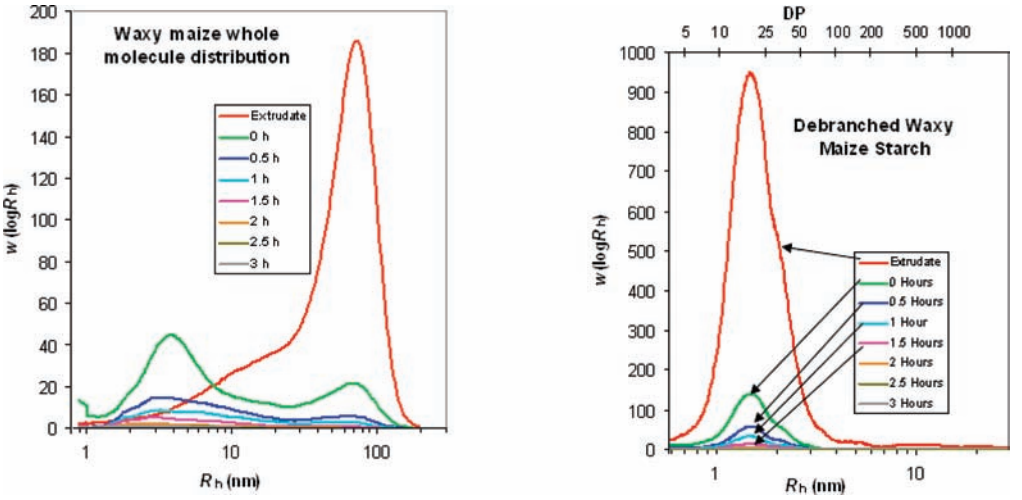

Figure 4. Data of **Figures 2** and **3** for waxy starch, plotted as two-dimensional distributions. For the debranched distributions, the degree of polymerization is also shown as the upper axis.

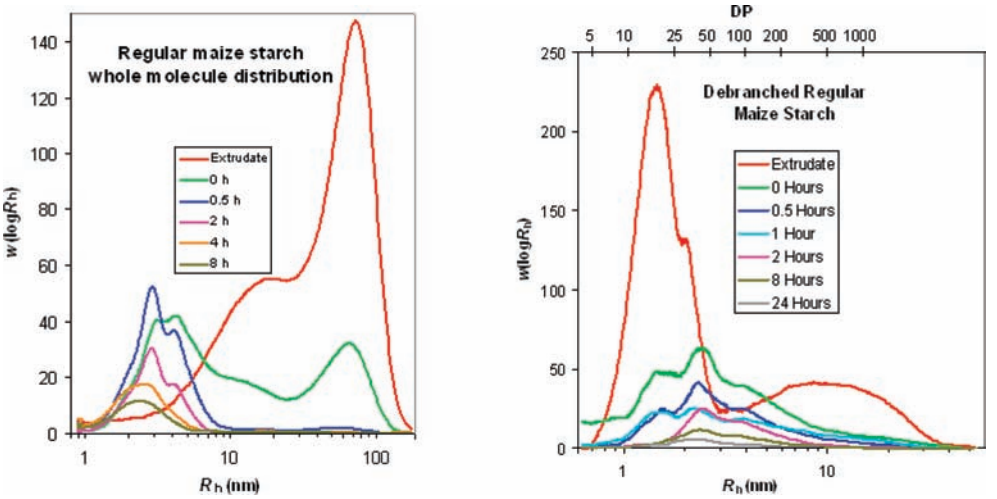

Figure 5. Data of **Figures 2** and **3** for rms, plotted as two-dimensional distributions. For the debranched distributions, the DP is also shown as the upper axis. The 24 h sample of the whole molecule distribution and the 4 h debranched distribution, shown in **Figures 2** and **3**, have been removed in this figure for clarity.

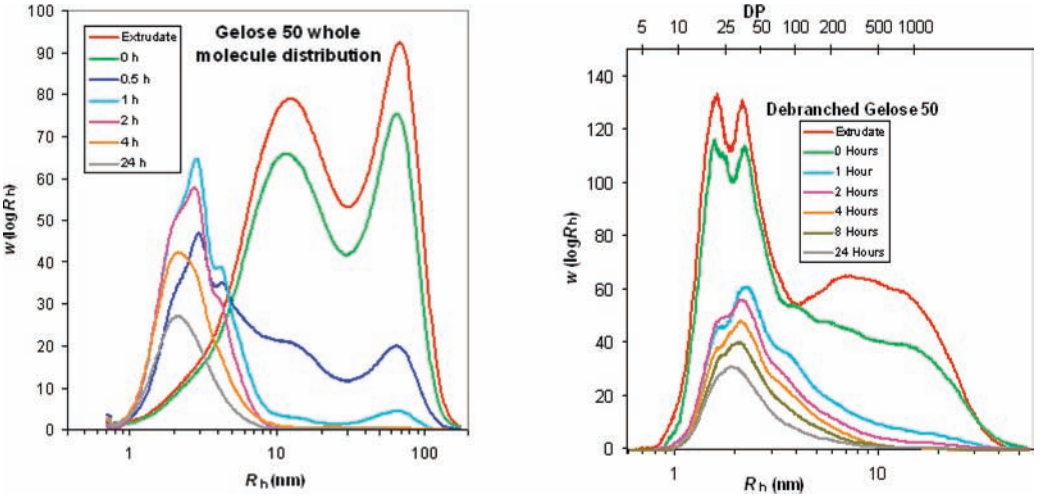

Figure 6. Data of **Figures 2** and **3** for Gelose 50, plotted as two-dimensional distributions. For the debranched distributions, the DP is also shown as the upper axis. The whole-molecule 8 h distribution is omitted for clarity.

symmetric more rapidly, after 4 h, than does that of Gelose 50, which becomes approximately symmetric only in the 24 h distribution. This indicates that the Gelose 80 more rapidly produces the remnant starch species, while more rapidly losing an additional molecular structure that is not involved in the final remnant starch species. Comparing the Gelose 50 to the rms

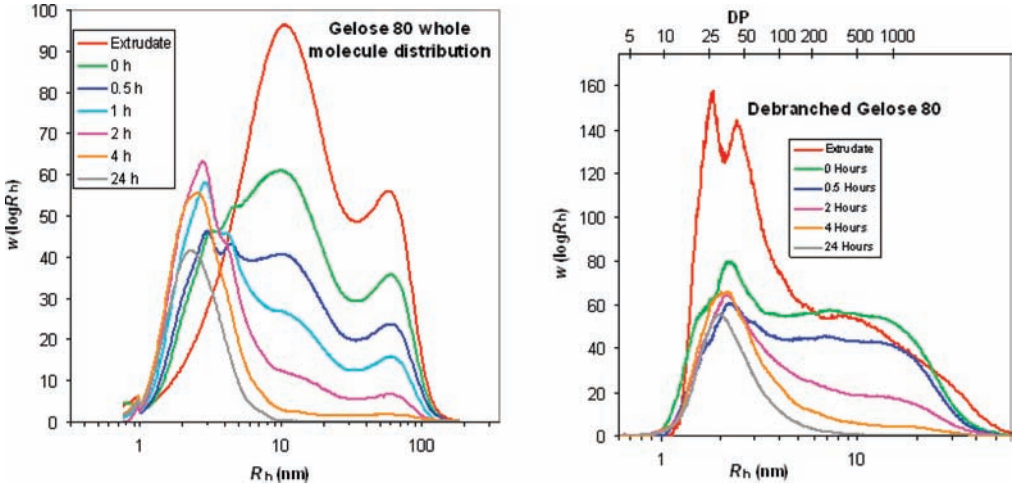

Figure 7. Data of **Figures 2** and **3** for Gelose 80, plotted as two-dimensional distributions. For the debranched distributions, the DP is also shown as the upper axis. The 8 h data, given in **Figures 2** and **3**, are omitted for clarity.

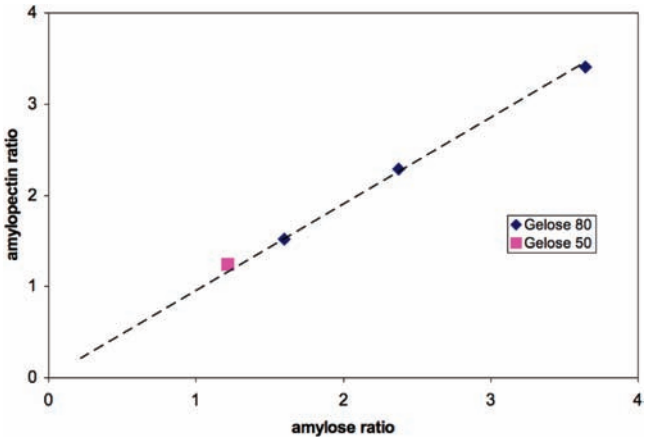

Figure 8. Ratios of the amounts of amylose and amylopectin for Gelose 50 and Gelose 80 at 0, 0.5, and 1 h to the amounts in the extrudate, measured by relative peak heights. The line is the least-squares fit, forced to pass through the origin.

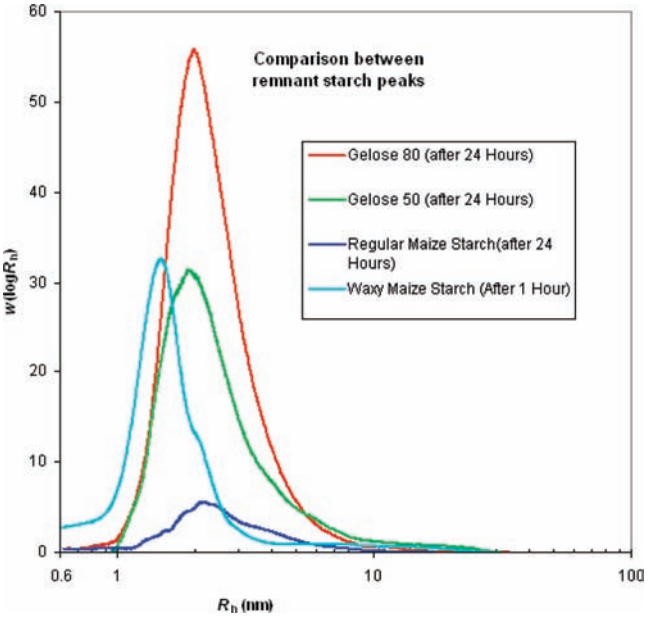

Figure 9. Comparison of 24 h debranched distributions for Gelose 80, Gelose 50, and rms.

shows that both achieve symmetry at about the same time, between 8 and 24 h of digestion. However, the rms remnant debranched distribution contains more peaks, probably from amylopectin, as seen in the waxy maize.

The first point to consider when interpreting these trends is that the ordering of (apparent) amylose content is Gelose 80 > Gelose 50 > rms > waxy maize. The other consideration is that the amylopectin structures of the parent amylopectin molecules in this study vary, with waxy maize showing the first debranched amylopectin peak of DP ~ 17, regular maize at DP ~17, Gelose 50 at DP ~ 20, and Gelose 80 at DP ~ 26 (**Figures 4**−**7**) . This shows the expected increase in amylopectin branch length, which accompanies the waxy mutation in high-amylose starch. The appearance of a predominantly linear remnant starch species that is common to all of the starches containing amylose and that was not present in the whole-molecule distributions (**Figure 2**), indicates that it is a product of the digestion process, while the varying amounts of the remnant starch species and its rate of production are determined by the molecular structure of the starting starch species. All of the remnant starch species display similar distributions even though they are produced from very different parent molecules. The comparison between the remnant species in Gelose 80, Gelose 50, regular and waxy maize starch, **Figure 9**, shows the similarity of the debranched remnant starch species in the three starches with significant amounts of amylose (i.e., all except waxy). The only requirement for the production of the remnant starch species seems to be that there is a population of linear starch chains that can be converted into the ~2 nm species. **Figure 5** shows the debranched rms remnant species overlapping mainly with the amylose portion (there is some minor overlapping with the amylopectin chains) of the extrudate sample. Gelose 80 and Gelose 50 debranched distributions display a significant overlap with the amylopectin portion of the extrudate sample. The differences in yield produced are probably due to an increasing population of starch chains long enough to form the remnant species. The correlation of apparent amylose with an increase in enzyme-resistant starch is explained by the increase in long chains that accompanies an increase in apparent amylose content.

Experiments by Eerlingen et al. (*16*) on a variety of amylose chain lengths found that a remnant starch species was produced with an average DP of 19−26 as determined via number-average end-group analysis. The starch species produced were independent

of the size of amylose chain from which it was produced, although an increase in remnant starch yield was observed with increasing amylose chain length. The current data show that the peak of the remnant starch species is at ~2 nm, equivalent to a DP of ~30 (calculated from the Mark−Houwink relation), and that with increasing apparent amylose content there is an increase in the yield of the remnant starch species. This shows a similarity between the results.

It is noted that residues produced by extensive acid hydrolysis have some similarity to those produced in the current experiment. Those residues frequently, although not always, show bimodal peaks, which when debranched become a single distribution of smaller chains, showing that acid hydrolysis produces branched remnants (*49*, *50*). This behavior bears some similarity to the digestion of extruded waxy maize, which produces a distribution of branched chains smaller than the parent molecules. There is not, however, a strong analogy between the acid-resistant fraction and the enzyme-resistant fragments produced in this study, as acid hydrolysis leaves significantly larger amounts of branching than observed in the present in vitro digestion.

These results can be used to produce a molecularly relevant definition of enzyme-resistant starch. The remnant starch species has a slower digestion rate than that of the whole starch molecules, and this decrease in digestion rate could potentially produce a significant increase in the amount of starch that passes through the small intestine to the large intestine. Thus, this remnant starch species is suggested to be responsible for the enzyme-resistant starch RS3.

The nature of the increase in apparent amylose may be deceptive, as in the case of high amylose maize an increase in apparent amylose content has been in part attributed to the increasing amylopectin chain lengths arising from a stronger expression of the amylose extender gene. The ability of the amylopectin fraction to produce a helical remnant starch population is likely to be lower than that of the amylose fraction, regardless of chain length, as the amylopectin has significantly more branching and thus is significantly more likely, if randomly attacked by α-amylase, to produce starch chains with branching points near the middle, which would cause an increase in helical imperfection. This is relevant when talking about the digestion and production of enzyme-resistant starch, as this production is strongly related to the kinetics of both digestion and the formation of starch helices as a process of retrogradation (*51*). Any branching points within the starch molecule will make producing a starch helix impossible unless the branching point can be excluded from the helical regions, that is, if the branch point is at the end of a starch helix, and thus not hindering helix formation (*52*). These caveats aside, it is possible, and perhaps likely, that the longer amylopectin chains are being made into linear starch chains and then forming helical enzyme-resistant starch.

In summary, this study focused on the digestion of a series of maize starches with differing levels of apparent amylose content. During the course of the digestion, a new starch species was produced, with a hydrodynamic radius of ~2 nm. This newly formed remnant starch species has a reduced digestion rate when compared to its parent molecules. The production of the remnant starch is due to the cleaving of long, mostly linear, chains into shorter, essentially linear, chains, which become more resistant to enzymatic digestion, presumably through the formation of helices. These largely linear chains come from both the amylose and the longer chains in amylopectin, particularly as present in the so-called high-amylose starches (Gelose 50 and Gelose 80).

This sheds light on the well-known correlation between higher levels of amylose and higher levels of resistant starch production. The amylose molecule is much more likely to have linear chains large enough to be cleaved into the lengths of unbranched starch that can form helices. In this study, it was observed that the high amylose starches Gelose 80 and Gelose 50 also had amylopectin branch lengths sufficient to form the remnant starch. It remains undetermined but likely that the long amylopectin chains characteristic of high amylose starches also contributed to enzyme-resistant starch formation.

LITERATURE CITED

(1) Buleon, A.; Colonna, P.; Planchot, V.; Ball, S. Starch granules: Structure and biosynthesis. *Int. J. Biol. Macromol.* **1998**, *23*, 85–112.

(2) WHO/FAO. *Carbohydrates in Human Nutrition*; WHO/FAO: Geneva, 1998.

(3) Topping, D. L.; Bajka, B. H.; Bird, A. R.; Clarke, J. M.; Cobiac, L.; Conlon, M. A.; Morell, M. K.; Toden, S. Resistant starches as a vehicle for delivering health benefits to the human large bowel. *Microb. Ecol. Health Dis.* **2008**, *20*, 103–108.

(4) Ao, Z.; Quezada-Calvillo, R.; Sim, L.; Nichols, B. L.; Rose, D. R.; Sterchi, E. E.; Hamaker, B. R. Evidence of native starch degradation with human small intestinal maltase-glucoamylase (recombinant). *FEBS Lett.* **2007**, *581*, 2381–2388.

(5) Behall, K., M; Hallfrisch, J. Plasma glucose and insulin reduction after consumption of breads varying in amylose content. *Eur. J. Clin. Nutr.* **2002**, *56*, 8.

(6) Behall, K. M.; Scholfield, D. J. Food amylose content affects postprandial glucose and insulin responses. *Cereal Chem.* **2005**, *82*, 654–659.

(7) Robertson, M. D.; Bickerton, A. S.; Dennis, A. L.; Vidal, H.; Frayn, K. N. Insulin-sensitizing effects of dietary resistant starch and effects on skeletal muscle and adipose tissue metabolism. *Am. J. Clin. Nutr.* **2005**, *82*, 559–567.

(8) Willis, H. J.; Eldridge, A. L.; Beiseigel, J.; Thomas, W.; Slavin, J. L. Greater satiety response with resistant starch and corn bran in human subjects. *Nutr. Res. (N.Y.)* **2009**, *29*, 100–105.

(9) Englyst, H. N.; Hudson, G. J. The classification and measurement of dietary carbohydrates. *Food Chem.* **1996**, *57*, 15–21.

(10) Topping, D. L.; Morell, M. K.; King, R. A.; Li, Z.; Bird, A. R.; Noakes, M. Resistant starch and health—*Himalaya 292*, a novel barley cultivar to deliver benefits to consumers. *Starch/Stärke* **2003**, *55*, 539–545.

(11) Bird, A. R.; Lopez-Rubio, A.; Shrestha, A. K.; Gidley, M. J. Resistant starch in vitro and in vivo: Factors determining yield, structure, and physiological relevance. In *Modern Biopolymer Science*; Kasapis, S., Norton, I. T., Ubbink, J. B., Eds.; Elsevier: London, 2009; pp 449−510.

(12) Berry, C. S. Resistant starch: Formation and measurement of starch that survives exhaustive digestion with amylolytic enzymes during the determination of dietary fibre. *J. Cereal Sci.* **1986**, *4*, 301–314.

(13) Sievert, D. P. Y. Enzyme-resistant starch. I. Characterization and evaluation by enzymatic, thermoanalytical, and microscopic methods. *Cereal Chem.* **1989**, *66*, 342–347.

(14) Gidley, M. J.; Cooke, D.; Darke, A. H.; Hoffmann, R. A.; Russell, A. L.; Greenwell, P. Molecular order and structure in enzyme-resistant retrograded starch. *Carbohydr. Polym.* **1995**, *28*, 23–31.

(15) Jiang, G.; Liu, Q. Characterization of residues from partially hydrolyzed potato and high amylose corn starches by pancreatic alpha-amylase. *Starch/Stärke* **2002**, *54*, 527–533.

(16) Eerlingen, R. C.; Deceuninck, M.; Delcour, J. A. Enzyme-resistant starch. II. Influence of amylose chain length on resistant starch formation. *Cereal Chem.* **1993**, *50*, 345–350.

(17) Salmeron, J.; Manson, J. E.; Stampfer, M. J.; Colditz, G. A.; Wing, A. L.; Willett, W. C. Dietary fiber, glycemic load, and risk of non-insulin-dependent diabetes mellitus in women. *J. Am. Med. Assoc.* **1997**, *277*, 472–477.

(18) Htoon, A.; Shrestha, A. K.; Flanagan, B. M.; Lopez-Rubio, A.; R. Bird, A.; Gilbert, E. P.; Gidley, M. J. Effects of processing high amylose maize starches under controlled conditions on structural organization and amylase digestibility. *Carbohydr. Polym.* **2009**, *75*, 236–245.

(19) Zhu, Q.; Bertoft, E. Composition and structural analysis of alpha-dextrins from potato amylopectin. *Carbohydr. Res.* **1996**, *288*, 155–174.
(20) Bertoft, E.; Boyer, C.; Manelius, R.; Avall, A.-K. Observations on the α-amylolysis pattern of some waxy maize starches from inbred line Ia453. *Cereal Chem.* **2000**, *77*, 657–664.
(21) Bertoft, E.; Manelius, R.; Myllärinen, P.; Schulman, A. H. Characterisation of dextrins solubilised by alpha-amylase from barley starch granules. *Starch/Stärke* **2000**, *52*, 160–163.
(22) Bertoft, E.; Zhu, Q.; Andtfolk, H.; Jungner, M. Structural heterogeneity in waxy-rice starch. *Carbohydr. Polym.* **1999**, *38*, 349–359.
(23) Hernández, O.; Emaldi, U.; Tovar, J. In vitro digestibility of edible films from various starch sources. *Carbohydr. Polym.* **2008**, *71*, 648–655.
(24) Kumari, M.; Urooj, A.; Prasad, N. N. Effect of storage on resistant starch and amylose content of cereal-pulse based ready-to-eat commercial products. *Food Chem.* **2007**, *102*, 1425–1430.
(25) Osorio-Díaz, P.; Bello-Pérez, L. A.; Agama-Acevedo, E.; Vargas-Torres, A.; Tovar, J.; Paredes-López, O. In vitro digestibility and resistant starch content of some industrialized commercial beans (*Phaseolus vulgaris* L.). *Food Chem.* **2002**, *78*, 333–337.
(26) Lopez-Rubio, A.; Htoon, A.; Gilbert, E. P. Influence of extrusion and digestion on the nanostructure of high-amylose maize starch. *Biomacromolecules* **2007**, *8*, 1564–1572.
(27) Zhang, G.; Ao, Z.; Hamaker, B. R. Nutritional property of endosperm starches from maize mutants: A parabolic relationship between slowly digestible starch and amylopectin fine structure. *J. Agric. Food Chem.* **2008**, *56*, 4686–4694.
(28) Zhang, G.; Sofyan, M.; Hamaker, B. R. Slowly digestible state of starch: mechanism of slow digestion property of gelatinized maize starch. *J. Agric. Food Chem.* **2008**, *56*, 4695–4702.
(29) Jiang, H.; Campbell, M.; Blanco, M.; Jane, J.-L. Characterization of maize amylose-extender (ae) mutant starches: Part II. Structures and properties of starch residues remaining after enzymatic hydrolysis at boiling-water temperature. *Carbohydr. Polym.* **2010**, *80*, 1–12.
(30) Evans, A.; Thompson, D. B. Enzyme susceptibility of high-amylose starch precipitated from sodium hydroxide dispersions. *Cereal Chem.* **2008**, *85*, 480–487.
(31) Poutanen, K.; Lauro, M.; Suortti, T.; Autio, K. Partial hydrolysis of gelatinized barley and waxy barley starches by alpha-amylase. *Food Hydrocolloids* **1996**, *10*, 269–275.
(32) Bertoft, E. Partial characterisation of amylopectin alpha-dextrins. *Carbohydr. Res.* **1989**, *189*, 181–193.
(33) Bertoft, E.; Manelius, R.; Myllarinen, P.; Schulman, A. H. Characterisation of dextrins solubilised by α-amylase from barley starch granules. *Starch/Staerke* **2000**, *52*, 160–163.
(34) Tan, I.; Flanagan, B. M.; Halley, P. J.; Whittaker, A. K.; Gidley, M. J. A method for estimating the nature and relative proportions of amorphous, single, and double-helical components in starch granules by 13C CP/MAS NMR. *Biomacromolecules* **2007**, *8*, 885–891.
(35) Champ, M.; Langkilde, A. M.; Brouns, F.; Kettlitz, B.; Le Bail-Collet, Y. Advances in dietary fibre characterisation. 2. Consumption, chemistry, physiology and measurement of resistant starch; implications for health and food labelling. *Nutr. Res. Rev.* **2003**, *16*, 143–161.
(36) Goni, I.; Garcia-Alonso, A.; Saura-Calixto, F. A starch hydrolysis procedure to estimate glycemic index. *Nutr. Res.* (*N.Y.*) **1997**, *17*, 427–437.
(37) O'Shea, M. G.; Samuel, M. S.; Konik, C. M.; Morell, M. K. Fluorophore-assisted carbohydrate electrophoresis (FACE) of oligosaccharides: efficiency of labelling and high-resolution separation. *Carbohydr. Res.* **1998**, *307*, 1–12.
(38) Schmitz, S.; Dona, A. C.; Castignolles, P.; Gilbert, R. G.; Gaborieau, M. Quantification of the extent of starch dissolution in dimethylsulfoxide by 1H NMR spectroscopy. *Macromol. Biosci.* **2009**, *9*, 506–514.
(39) Morell, M. K.; Samuel, M. S.; O'Shea, M. G. Analysis of starch structure using fluorophore-assisted carbohydrate electrophoresis. *Electrophoresis* **1998**, *19*, 2603–2611.
(40) Cave, R. A.; Seabrook, S. A.; Gidley, M. J.; Gilbert, R. G. Characterization of starch by size-exclusion chromatography: The limitations imposed by shear scission. *Biomacromolecules* **2009**, *10*, 2245–2253.
(41) Bianchi, U.; Peterlin, A. Intrinsic viscosity of polymers of low molecular weight. *J. Polym. Sci., Polym. Phys. Ed.* **1968**, *6*, 1759–1772.
(42) Liu, W.-C.; Halley, P. J.; Gilbert, R. G. Mechanism of degradation of starch, a highly branched polymer, during extrusion. *Macromolecules* **2010**, *43*, 2855–2864.
(43) Jane, J.; Chen, Y. Y.; Lee, L. F.; McPherson, A. E.; Wong, K. S.; Radosavljevic, M.; Kasemsuwan, T. Effects of amylopectin branch chain length and amylose content on the gelatinization and pasting properties of starch. *Cereal Chem.* **1999**, *76*, 629–637.
(44) Meira, G.; Netopilik, M.; Potschka, M.; Schnoll-Bitai, I.; Vega, J. Band broadening function in size exclusion chromatography of polymers: review of some recent developments. *Macromol. Symp.* **2007**, *258*, 186–197.
(45) Yao, Y.; Thompson, D. B.; Guiltinan, M. J. Maize starch-branching enzyme isoforms and amylopectin structure. In the absence of starch-branching enzyme IIb, the further absence of starch-branching enzyme Ia leads to increased branching. *Plant Physiol.* **2004**, *136*, 3515–3523.
(46) Klucinec, J. D.; Thompson, D. B. Structure of amylopectins from ae-containing maize starches. *Cereal Chem.* **2002**, *79*, 19–23.
(47) Lauro, M.; Forsell, P. M.; Suortti, M. T.; Hulleman, S. H. D.; Poutanen, K. S. α-Amylolysis of large barley starch granules. *Cereal Chem.* **1999**, *76*, 925–930.
(48) Manelius, R.; Bertoft, E. The effect of Ca^{2+}-ions on the [alpha]-amylolysis of granular starches from oats and waxy-maize. *J. Cereal Sci.* **1996**, *24*, 139–150.
(49) Gérard, C.; Colonna, P.; Buléon, A.; Planchot, V. Order in maize mutant starches revealed by mild acid hydrolysis. *Carbohydr. Polym.* **2002**, *48*, 131–141.
(50) Jacobs, H.; Eerlingen, R. C.; Rouseu, N.; Colonna, P.; Delcour, J. A. Acid hydrolysis of native and annealed wheat, potato and pea starches—DSC melting features and chain length distributions of lintnerised starches. *Carbohydr. Res.* **1998**, *308*, 359–371.
(51) Lopez-Rubio, A.; Flanagan, B. M.; Shrestha, A. K.; Gidley, M. J.; Gilbert, E. P. Molecular rearrangement of starch during in vitro digestion: Toward a better understanding of enzyme resistant starch formation in processed starches. *Biomacromolecules* **2008**, *9*, 1951–1958.
(52) Yamamoto, T.; Orimi, N.; Urakami, N.; Sawada, K. Molecular dynamics modeling of polymer crystallization; from simple polymers to helical ones. *Faraday Discuss.* **2005**, *128*, 75–86.

Received for review March 22, 2010. Revised manuscript received June 7, 2010. Accepted June 14, 2010. We gratefully acknowledge the financial support of a Discovery Grant from the Australian Research Council (DP0985694) and of a grant from the Australian Institute for Nuclear Science & Engineering.